Equation of State of Nuclear Matter in 158*A* GeV Pb + Pb Collisions

B. R. Schlei,[1,*] D. Strottman,[1,†] and N. Xu[2,‡]

[1]*Theoretical Division, Los Alamos National Laboratory, Los Alamos, New Mexico 87545*
[2]*Nuclear Science Division, Lawrence Berkeley Laboratory, Berkeley, California 94720*

(Received 21 October 1997)

Within a hydrodynamical approach we investigate the sensitivity of single inclusive momentum spectra of hadrons in 158*A* GeV Pb + Pb collisions to three different equations of state of nuclear matter. The initial conditions before the evolution of the fireballs and the space-time evolution pictures differ dramatically for the three equations of state when the same freeze-out temperature is used in all calculations. However, the softest of the equations of state results in transverse mass spectra that are too steep in the central rapidity region. We conclude that the transverse particle momenta are determined by the effective softness of the equation of state during the fireball expansion. [S0031-9007(98)05858-X]

PACS numbers: 24.10.Jv, 21.65.+f, 24.85.+p, 25.75.–q

A goal of studying ultrarelativistic heavy ion collisions is to understand nuclear matter under extreme conditions such as high energy density, high particle density, and whether a transition from a quark-confined hadron state to the deconfined state (quark-gluon plasma, QGP) takes place (see, e.g., Ref. [1]). A highly excited state of matter and a possible transition to a QGP will occur at the early stages of the heavy-ion collisions; these differences will be reflected in different equations of state for nuclear matter. These in turn will affect the maximum energy density and compression achieved in a heavy ion reaction. To investigate the nature of the hadronic equation of state and possible phase transitions, it is very important to obtain information about the conditions that exist at maximum compression, the subsequent evolution of the system, and the final free hadrons that can be measured in the detectors.

The equation of state (EOS) is part of a hydrodynamic model, and the connection between the EOS and experimental observables is relatively direct. In order to address issues raised above, we shall use the simulation code HYLANDER-C (cf. Ref. [2], and references therein), with different equations of state and Cooper-Frye freeze-out [3], to predict the single particle momentum distributions. The experimental spectra from the 158*A* GeV Pb + Pb collisions, measured by the NA44 [4,5] and NA49 Collaborations [6], are used as fit criteria for the hydrodynamical (one-fluid-type) calculations.

In our approach, virtually any type of EOS can be considered by solving the relativistic Euler equations [7]. The coupled system of partial differential equations necessary that describe the dynamics of a relativistic fluid (with given initial conditions) contains an equation of state which we write in the form

$$P(\epsilon, n) = c^2(\epsilon, n)\epsilon\,. \tag{1}$$

In Eq. (1), the quantities P, ϵ, and n are the pressure, the energy density, and the baryon density, respectively. The proportionality constant, c^2, is in general a function of ϵ and n. In the following, we shall assume that in particular the n dependence is negligible for the energy regime under consideration. From only the knowledge of the speed of sound, $c_0^2(\epsilon)$, one can then calculate $c^2(\epsilon)$ by evaluating the integral [8]

$$c^2(\epsilon) = \frac{1}{\epsilon}\int_0^{\epsilon} c_0^2(\epsilon')\,d\epsilon'. \tag{2}$$

Assuming an adiabatic expansion, the temperature, $T(\epsilon)$, can be calculated from [8]

$$T(\epsilon) = T_0 \exp\left[\int_{\epsilon_0}^{\epsilon} \frac{c_0^2(\epsilon')\,d\epsilon'}{[1 + c^2(\epsilon')]\epsilon'}\right], \tag{3}$$

where $T_0 = T(\epsilon_0)$ has to be specified for an arbitrary value of ϵ_0.

Three equations of state are discussed in this study. The first one, EOS-I, which we use in the following, exhibits a phase transition to a quark-gluon plasma at a critical temperature $T_c = 200$ MeV with a critical energy density $\epsilon_c = 3.2$ GeV/fm^3 (cf. Ref. [9], and references therein [2]). The second equation of state, EOS-II, is also a lattice QCD-based EOS which has recently become very popular in the field of relativistic heavy-ion physics (cf. Ref. [10]). This equation of state includes a phase transition at $T_c = 160$ MeV with a critical energy density $\epsilon_c \approx 1.5$ GeV/fm^3. The third equation of state, EOS-III, has been extracted from the microscopic transport model RQMD [11] under the assumption of complete local thermalization [12], and does *not* include a transition to a QGP. In Fig. 1 the three equations of state are plotted in many different representations. For instance, in Fig. 1(d) the plot of $c^2 = P(\epsilon)/\epsilon$ emphasizes the existence of a minimum in P/ϵ at $\epsilon = \epsilon_c = 3.2$ GeV/fm^3 ($\approx$1.5 GeV/fm^3) for EOS-I (EOS-II), referred to as *the softest point* of the EOS. It corresponds to the boundary between the generalized mixed phase and the QGP [10]. As seen in Fig. 1, EOS-II yields a much softer equation of state than does EOS-I.

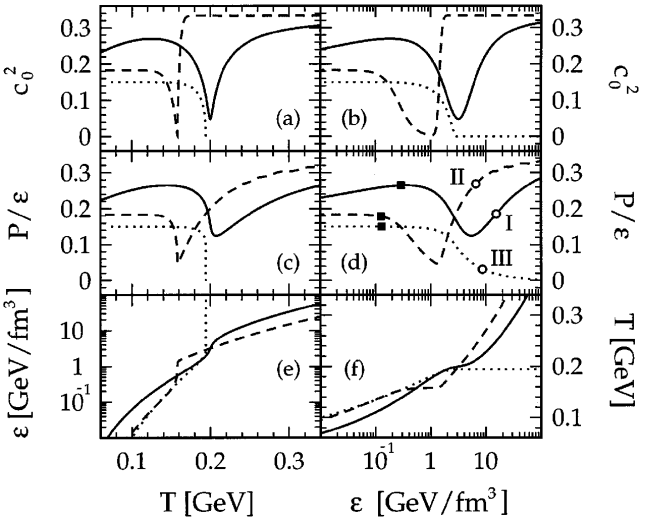

FIG. 1. Energy density, ϵ, ratio of pressure and energy density, P/ϵ, speed of sound, c_0^2, and temperature, T, as functions of T and/or ϵ, for the equations of state EOS-I (solid lines), EOS-II (dashed lines), and EOS-III (dotted lines), respectively (see text). The open circles in plot (d) correspond for each EOS to the starting values of P/ϵ with respect to the achieved initial maximum energy density ϵ_Δ at transverse position $r_\perp = 0$, whereas the filled squares represent the final values of P/ϵ at breakup energy densities, ϵ_f.

The parametrizations for the speed of sound which we have used here are [8]

$$c_0^2(\epsilon) = \{\alpha + \beta \tanh[\gamma \ln(\epsilon/\epsilon_0) + \delta]\} \times \left[1 - \frac{(1-\xi)\Gamma^2}{\ln^2(\epsilon/\epsilon_0) + \Gamma^2}\right] \quad (4)$$

in the case of EOS-I,

$$c_0^2(\epsilon) = \alpha + \beta \tanh[\gamma \ln(\epsilon/\epsilon_0)] - \delta \tanh[\xi \ln(\epsilon/\epsilon')] \quad (5)$$

in the case of EOS-II, and

$$c_0^2(\epsilon) = \begin{cases} \alpha - \beta(\epsilon/\epsilon_0)^\delta: & \epsilon \le \epsilon', \\ 0: & \epsilon > \epsilon' \end{cases} \quad (6)$$

in the case of EOS-III. The parameters of Eqs. (4)–(6) and the choices for $T_0 = T(\epsilon_0)$ are listed in Table I.

In the following it is assumed that due to an experimental uncertainty for the centrality of the collision, only 90% of the total available energy and the total baryon number have been observed. It is then possible to find initial distributions for the three equations of state, such that one can reproduce the single inclusive momentum spectra of 158A GeV Pb + Pb collisions (cf. Fig. 3).

Figure 2 shows the initial distributions for the energy density, $\epsilon(z)$, the baryon density, $n_B(z)$, and the fluid rapidity, $y_F(z)$, plotted against the longitudinal coordinate z. We use here for the initial distributions the initial condition scenarios which have been extensively described in Refs. [13,14]. In particular, it is assumed

TABLE I. EOS Parameters.

	EOS-I	EOS-II	EOS-III
α	4/15	0.2582	0.15
β	1/15	1/6	0.02
γ	0.24	10.0	...
δ	1.05	0.0915	2.00
ξ	0.15	1.50	...
Γ^2	0.73	...	...
ϵ' [GeV/fm^3]	...	0.27	2.80
ϵ_0 [GeV/fm^3]	3.20	1.45	1.00
T_0 [MeV]	200	160	180

that an initial transverse fluid velocity field is absent, and the initial longitudinal distributions for energy density, ϵ, and baryon density, n_B, are smeared out with a Woods-Saxon parametrization in the transverse direction, $r_\perp$ (cf. Ref. [15]). The choices for the initial parameters, which in each case provide the best fit results for the hadronic single inclusive momentum spectra of the two considered experiments, are listed in Table II.

The maximum initial energy density is $\epsilon_\Delta = 15.3\ [6.55\ (8.66)]$ GeV/fm^3, and the maximum initial baryon density is $n_B^{\max} = 3.93\ [1.24\ (1.92)]$ fm^{-3}, for EOS-I [EOS-II (EOS-III)], respectively; 71% [30% (36%)] of the baryonic matter is initially located in the central fireball region. Hence, EOS-I predicts a much larger stopping than EOS-III does, and EOS-III predicts a much larger stopping than EOS-II does.

Figure 3 shows results of the hydrodynamical calculations compared to the single inclusive momentum spectra of the 158A GeV Pb + Pb collisions which have been measured by the NA44 [4,5] and NA49 Collaborations [6]. All single inclusive momentum spectra have been evaluated in the nucleus-nucleus center of mass system ($y_{\text{c.m.}} = 2.91$), and for all calculations the freeze-out temperature $T_f = 139$ MeV has been used. The energy density at freeze-out is $\epsilon_f = 0.292\ [0.126\ (0.130)]$ GeV/fm^3 for EOS-I [EOS-II (EOS-III)]. In particular, the freeze-out energy density, ϵ_f, is a factor $\sim$2.2 larger in the calculation

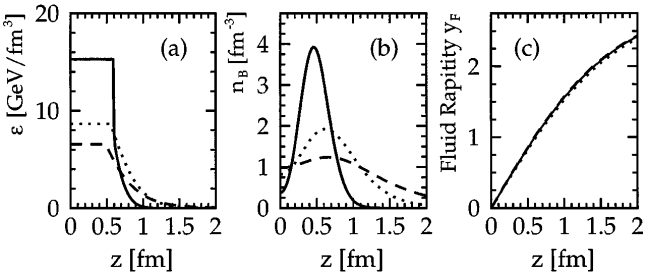

FIG. 2. Initial distributions of (a) the energy density, ϵ, (b) the baryon density, n_B, and (c) the fluid rapidity, y_F, plotted against the longitudinal coordinate z at transverse position $r_\perp = 0$. The solid [dashed (dotted)] lines indicate the initial distributions for the calculation using EOS-I [EOS-II (EOS-III)].

TABLE II. Properties of the fireballs.

	EOS-I	EOS-II	EOS-III
Initial parameters			
Relative fraction of thermal energy in the central fireball, K_L	0.55	0.20	0.28
Longitudinal extension of the central fireball, Δ [fm]	1.20	1.00	1.10
Rapidity at the edge of the central fireball, y_Δ	1.00	0.85	0.90
Rapidity at maximum of initial baryon y distribution, y_m	0.80	1.50	1.10
Width of initial baryon y distribution, σ	0.32	1.00	0.60
Output			
Maximum initial energy density, ϵ_Δ [GeV/fm^3]	15.3	6.55	8.66
Maximum initial baryon density, $n_B^{\max}$ [fm^{-3}]	3.93	1.24	1.92
Relative fraction of baryons in central fireball, $f_{n_B}^\Delta$	0.71	0.30	0.36
Freeze-out energy density, ϵ_f [GeV/fm^3]	0.292	0.126	0.130
Maximum transverse velocity at freeze-out, $v_\perp^{\max}$ [c]	0.46	0.30	0.42
Lifetime of fireball, $t_{\max}$ [fm/c]	13.1	29.3	27.3
Lifetime of QGP, $t_{\rm QGP}$ [fm/c]	2.4	3.0	...

using EOS-I compared to the other two calculations. Inspecting Fig. 4, we found that the total lifetime of the fireball is reduced by approximately this factor in the calculation using EOS-I. Figure 4 also shows that EOS-II and EOS-III yield fireballs of similar lifetimes (cf. also Table II). These particular features show up in Bose-Einstein correlation (BEC) calculations (cf. Ref. [2]); more on BEC will be published elsewhere [16]. The relatively strong effect in two-particle correlation functions was also observed in a recent report [17].

All three calculations yield reasonable agreement with both experiments. However, the calculations for the very soft EOS-II yield transverse mass spectra that are too steep in the central rapidity region. The magnitudes of the slopes in the transverse mass spectra have their origin in the transverse velocity fields at freeze-out. For EOS-II its corresponding transverse velocity field is the weakest (cf. Table II) of the three EOS. In fact, it is about 30% smaller than the transverse velocity fields for EOS-I and EOS-III. The final velocity is proportional to the time integral

$$\int_{t_i}^{t_f} \frac{P}{\epsilon}(t')\,dt', \tag{7}$$

where P/ϵ is proportional to the fluid acceleration [18,19]. In Fig. 1(d) we exhibit for each EOS we used the starting values of P/ϵ with respect to the initial maximum energy density ϵ_Δ at transverse position $r_\perp = 0$, and the final values of P/ϵ at breakup energy densities,

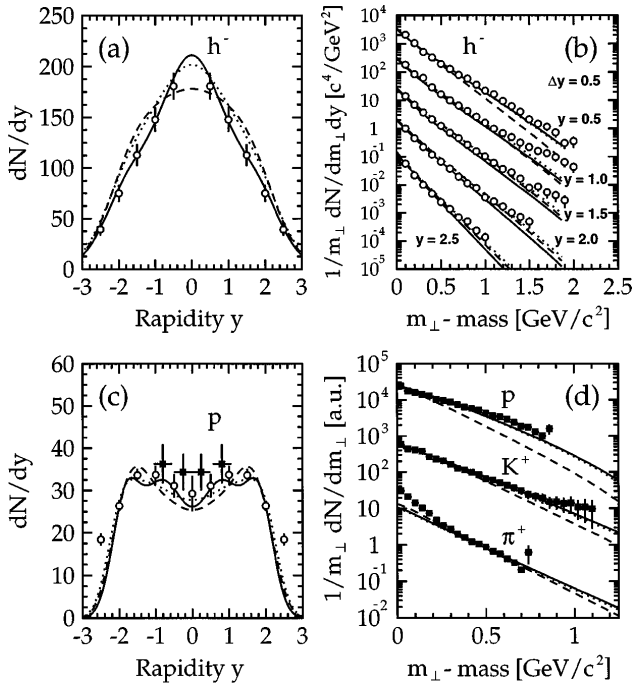

FIG. 3. (a) Rapidity spectra and (b) transverse mass spectra, $(1/m_\perp)dN/dm_\perp dy$, of negative hadrons, h^-, (c) rapidity spectra of protons (without contributions from Λ^0 decay) and (d) transverse mass spectra, $(1/m_\perp)dN/dm_\perp$, of protons (including contributions from Λ^0 decay), p, positive kaons, K^+, and positive pions, π^+, respectively. The solid [dashed (dotted)] lines indicate the results of the calculations when using equation of state EOS-I [EOS-II (EOS-III)]. The open circles represent preliminary data taken by the NA49 Collaboration, whereas the filled squares represent final data taken by the NA44 Collaboration.

ϵ_f. For the given total fireball lifetime, $t_{\max} \equiv t_f - t_i$, the effective P/ϵ of EOS-II is obviously too small, whereas P/ϵ of EOS-I and EOS-III appear to have the correct effective softness. We stress that the total lifetime, $t_{\max}$, in the case of EOS-I is reduced by a

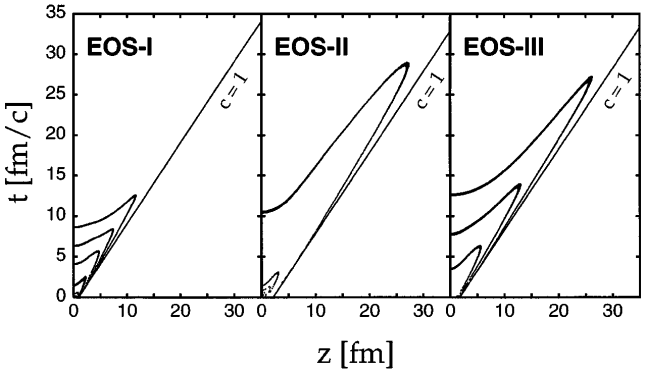

FIG. 4. Isotherms for the relativistic fluids governed by EOS-I, EOS-II, and EOS-III at $r_\perp = 0$, respectively. The outer lines correspond to a temperature, $T = 139$ MeV, and each successively smaller curve represents an increase in temperature by $\Delta T = 20$ MeV. The lines $c = 1$ represent the light cone.

factor ~ 2.1 compared to $t_{\max}$ of EOS-III, but the ratio P/ϵ of EOS-I is effectively increased for the considered expansion period.

In summary, we have tested three types of equation of state for 158A GeV Pb + Pb collisions. We found that the measured single inclusive momentum spectra are sensitive to both the initial conditions and to the equation of state. EOS-I and EOS-III both provide reasonable fits to the data. For the EOS-II a softest point is assumed and its corresponding velocity field is the weakest. As a result, the transverse mass distributions calculated from this equation of state are found to be too steep in the central rapidity region as compared to the experimental observations. Obviously, the transverse particle momenta are sensitive to the effective softness of the equation of state during the fireball expansion.

We stress that we have based our considerations on very strong assumptions. In the calculations we are using an idealized hadronization criterion (i.e., $T_f = 139$ MeV for all hadron species), idealized equations of state (i.e., not n dependent), ideal fluid dynamics (i.e., nonviscous), and an idealized link between quantum statistics and (classical) relativistic fluid dynamics (i.e., particle spectra have been calculated from Wigner functions). But as long as we limit our comparison of different scenarios within the same framework, our conclusions are valid. Still, several crucial questions like where and when the collective velocity field [20] is developed during the collision, and whether it develops in the QGP phase or in the hadronic phase are not answered yet. In addition, the exact condition for the system evolving from interacting hadrons to freeze-streaming ones is not known [21]. To shed light in this direction, an even more sophisticated analysis is needed. We believe that the combined analysis of single inclusive momentum spectra and Bose-Einstein correlations will help to further constrain [22] the limits of possible candidates for the equation of state of nuclear matter in relativistic heavy-ion collisions.

We thank Dr. H. Sorge for providing us all the necessary information for the construction of the RQMD EOS. We are grateful for many enlightening discussions with Dr. M. Prakash, Dr. C. Redlich, Dr. D. Rischke, Dr. E. V. Shuryak, and Dr. H. Sorge. Special thanks goes to M. Toy for providing us data files of the preliminary NA49 data. This work has been supported by the U.S. Department of Energy.

*Electronic address: schlei@LANL.gov
†Electronic address: dds@LANL.gov
‡Electronic address: nxu@LBL.gov

[1] *Quark Matter '96, Proceedings of the Twelfth International Conference on Ultra-Relativistic Nucleus-Nucleus Collisions, Heidelberg, Germany, 1996*, edited by P. Braun-Munzinger, H. J. Specht, R. Stock, and H. Stöcker [Nucl. Phys. **A610**, 1c–572c (1996)].
[2] B. R. Schlei, Heavy Ion Phys. **5**, 403 (1997).
[3] F. Cooper, G. Frye, and E. Schonberg, Phys. Rev. D **11**, 192 (1975).
[4] NA44 Collaboration, I. G. Bearden *et al.*, Phys. Rev. Lett. **78**, 2080 (1997); NA44 Collaboration, Nu Xu *et al.*, in Ref. [1], p. 175c.
[5] NA44 Collaboration, I. G. Bearden *et al.*, Phys. Lett. B **388**, 431 (1996).
[6] NA49 Collaboration, P. G. Jones *et al.*, in Ref. [1], p. 188c.
[7] L. D. Landau and E. M. Lifschitz, *Fluid Mechanics* (Pergamon, New York, 1959).
[8] U. Ornik, Ph.D. thesis, Universität Marburg, 1990.
[9] K. Redlich and H. Satz, Phys. Rev. D **33**, 3747 (1986).
[10] C. M. Hung and E. V. Shuryak, Phys. Rev. Lett. **75**, 4003 (1995).
[11] RQMD = relativistic quantum molecular dynamics. For details of the model, see, e.g., A. von Keitz *et al.*, Phys. Lett. B **263**, 353 (1991); H. Sorge *et al.*, Phys. Lett. B **289**, 6 (1992); H. Sorge, Phys. Rev. C **52**, 3291 (1995).
[12] H. Sorge, Phys. Lett. B **402**, 251 (1997).
[13] U. Ornik, M. Plümer, B. R. Schlei, D. Strottman, and R. M. Weiner, Phys. Rev. C **54**, 1381 (1996).
[14] J. Bolz, U. Ornik, and R. M. Weiner, Phys. Rev. C **46**, 2047 (1992).
[15] J. Bolz, U. Ornik, M. Plümer, B. R. Schlei, and R. M. Weiner, Phys. Rev. D **47**, 3860 (1993).
[16] B. R. Schlei (to be published).
[17] M. Gyulassy, D. Rischke, and B. Zhang, Nucl. Phys. **A613**, 613 (1997).
[18] E. V. Shuryak and O. V. Zhirov, Phys. Lett. **89B**, 253 (1980).
[19] E. V. Shuryak, "The Phases of QCD," in Proceedings of the RHIC Summer Studies, Brookhaven, 1996, hep-ph/9609249; Heavy Ion Phys. **5**, 395 (1997)
[20] H. von Gersdorff, L. D. McLerran, M. Kataja, and P. V. Ruuskanen, Phys. Rev. D **34**, 794 (1986).
[21] H. Sorge, Phys. Lett. B **373**, 16 (1996).
[22] D. Ferenc, in Ref. [1], p. 523c.